Concerted Action of PGC-1-related Coactivator (PRC) and c-MYC in the Stress Response to Mitochondrial Dysfunction[*]

Natalie Gleyzer and Richard C. Scarpulla[1]

From the Department of Cell and Molecular Biology, Northwestern Medical School, Chicago, Illinois 60611

Edited by John Denu

PGC-1-related coactivator (PRC) has a dual function in growth-regulated mitochondrial biogenesis and as a sensor of metabolic stress. PRC induction by mitochondrial inhibitors, intracellular ROS, or topoisomerase I inhibition orchestrates an inflammatory program associated with the adaptation to cellular stress. Activation of this program is accompanied by the coordinate expression of c-MYC, which is linked kinetically to that of PRC in response to multiple stress inducers. Here, we show that the c-MYC inhibitor 10058-F4 blocks the induction of c-MYC, PRC, and representative PRC-dependent stress genes by the respiratory chain uncoupler, carbonyl cyanide *m*-chlorophenyl hydrazine (CCCP). This result, confirmed by the suppression of PRC induction by c-MYC siRNA silencing, demonstrates a requirement for c-MYC in orchestrating the stress program. PRC steady-state expression was markedly increased upon mutation of two GSK-3 serine phosphorylation sites within the carboxyl-terminal domain. The negative control of PRC expression by GSK-3 was consistent with the phosphor-inactivation of GSK-3β by CCCP and by the induction of PRC by the GSK-3 inhibitor AZD2858. Unlike PRC, which was induced post-translationally through increased protein half-life, c-MYC was induced predominantly at the mRNA level. Moreover, suppression of Akt activation by the Akt inhibitor MK-2206 blocked the CCCP induction of PRC, c-MYC, and representative PRC stress genes, demonstrating a requirement for Akt signaling. MK-2206 also inhibited the phosphor-inactivation of GSK-3β by CCCP, a result consistent with the ability of Akt to phosphorylate, and thereby suppress GSK-3 activity. Thus, PRC and c-MYC can act in concert through Akt-GSK-3 signaling to reprogram gene expression in response to mitochondrial stress.

PRC[2] is a structurally and functionally unique member of the PGC-1 family of regulated coactivators (1, 2). These coactivators can direct programs of gene expression in response to extracellular signals that govern multiple metabolic functions.

PRC mRNA is induced by serum growth factors in the absence of *de novo* protein synthesis (3) placing the PRC gene (*PPRC1*) in the class of immediate early or primary response genes (4–6). Efficient PRC silencing in cultured human cells led to severe respiratory chain dysfunction accompanied by abundant atypical mitochondria (1, 7). This classic mitochondrial loss of function phenotype was also observed upon tissue-specific disruption of several nuclear genes whose products are required by the mitochondrial genetic system (8–10). PRC is unique among PGC-1 family members in that mice with a germ line knock-out of *PPRC1* exhibited early embryonic lethality (11), a phenotype common to mouse knockouts of NRF-1, NRF-2, YY1, and other factors associated with the maintenance of mitochondrial function (12, 13). Thus, PRC serves a distinct function in linking the cell growth program to the biogenesis of mitochondria (3, 14).

In addition to its metabolic regulatory role, PRC is required for the induction of an inflammatory/stress response to multiple metabolic insults (15, 16). Under conditions of mitochondrial impairment or replication stress, PRC orchestrates a program of inflammatory gene expression associated with apoptosis, premature senescence, and metabolic reprogramming (15, 16). Induction of PRC and the PRC stress genes occurred in response to mechanistically diverse inhibitors of mitochondrial function including the respiratory chain uncouplers CCCP and DNP, a dominant negative allele of NRF-1, which inhibits mitochondrial biogenesis (17), and meclizine, a respiratory chain inhibitor that directs a shift to glycolytic metabolism (18). PRC induction coincides with the up-regulation of multiple genes associated with the adaptive response to cellular dysfunction including pro-survival inflammatory mediators and anti-apoptotic factors (15). Several genes of this adaptive response overlap with genes of the inflammatory program of senescent cells and with inflammatory genes expressed in tumor microenvironments (15, 16). The results demonstrate that PRC is an essential component of a mechanism that reprograms nuclear gene expression in response to mitochondrial stress.

A consistent feature of the PRC-dependent program is the tight coordinate regulation of PRC and c-MYC protein expression. In contrast to several other transcription factors associated with the nuclear control of mitochondrial function, c-MYC was coordinately up-regulated with PRC in response to the respiratory chain uncoupler CCCP (15). In addition, PRC and c-MYC were induced coordinately by intracellular ROS production leading to apoptosis and to the induction of premature senescence through topoisomerase I inhibition (16). More-
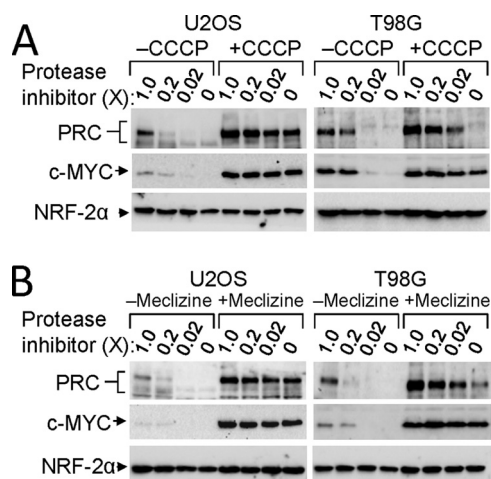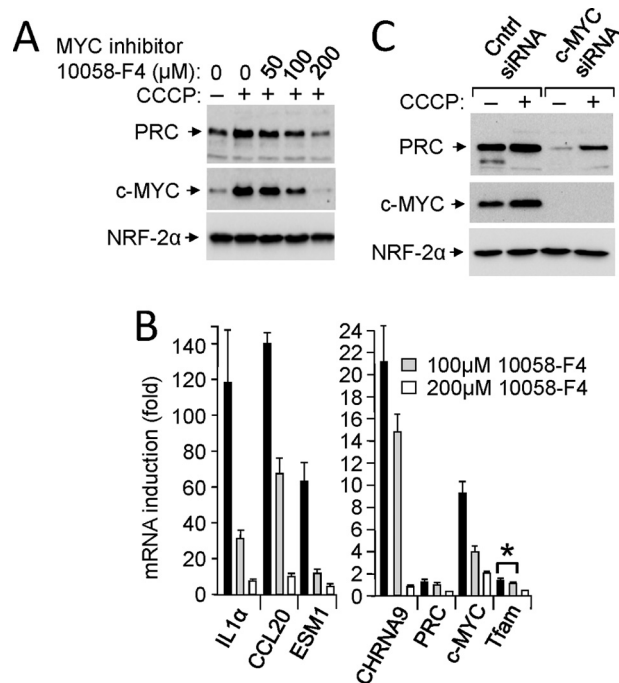
FIGURE 1. **Inducer-dependent protease resistance of PRC and c-MYC.** *A,* human log phase U2OS or T98G cells were plated and 24–48 h later were treated with either vehicle (−) or CCCP (+) for 24 h. Total cell extracts from subconfluent cells were prepared using the indicated dilution (*X*) of protease inhibitor mixture and subjected to immunoblotting using rabbit anti-PRC(1047–1379), mouse anti-c-MYC, or rabbit anti-NRF-2α antibodies. *B,* human log phase U2OS or T98G cells were plated as in *A* and treated with either vehicle (−) or meclizine (+) for 48 h. Total cell extracts from subconfluent cells were prepared and subjected to immunoblotting as in *A.*

FIGURE 2. **Suppression of the PRC stress program by c-MYC inhibitor.** *A,* human log phase U2OS cells were plated as in Fig. 1*A* and treated with vehicle or CCCP in the presence of the indicated concentration of the c-MYC inhibitor 10058-F4. Total cell extracts from subconfluent cells were prepared and subjected to immunoblotting using rabbit anti-PRC, mouse anti-c-MYC, or rabbit anti-NRF-2α antibodies. *B,* total RNA was prepared from log phase U2OS cells treated as in *A.* The fold induction by CCCP in the presence of the indicated concentrations of 10058-F4 of the PRC stress genes (*IL1α, CCL20, ESM1,* and *CHRNA9*) compared with that of *PRC, Tfam,* and *c-MYC* was determined by quantitative real time PCR. RNA induction for each gene is expressed relative to the untreated control. The values are the averages ± S.E. for at least three independent experiments with a minimum of two technical replicas for each determination. Differences with a *p* value >0.05 were taken as statistically insignificant as indicated by *asterisk.* *C,* human log phase U2OS cells were transfected with either control siRNA or c-MYC siRNA and treated 48 h post-transfection with either vehicle or CCCP for 16 h. Total cell extracts were prepared and subjected to immunoblotting using rabbit anti-PRC, mouse anti-c-MYC, or rabbit anti-NRF-2α antibodies.

over, the induction of PRC, c-MYC, and the PRC stress genes all showed the same antioxidant sensitivities depending upon the ROS dependence of the inducer. CCCP and menadione treatment led to the antioxidant-sensitive induction of PRC, c-MYC, and the stress genes, whereas the induction of all three by SN-38 was unaffected by antioxidant, suggesting that ROS-dependent and -independent stress pathways converge on PRC and c-MYC. The striking coordination of PRC and c-MYC induction by multiple stress inducers and their identical antioxidant sensitivities suggested that PRC and c-MYC are part of the same cellular stress pathway.

Here, we explore the molecular mechanisms mediating the coordinate induction of PRC and c-MYC in response to mitochondrial stress. The results demonstrate that PRC induction by CCCP is coordinated with that of c-MYC through Akt-GSK-3 signaling that targets tandem GSK-3 consensus phosphorylation sites within the PRC carboxyl-terminal domain.

Results

A Requirement for c-MYC in the Coordinate Induction of PRC—PRC and c-MYC protein induction occurs in response to mechanistically distinct inhibitors of mitochondrial biogenesis and function (15, 16). The steady-state expression of both proteins is highly sensitive to the inclusion of protease inhibitors in the cell lysis buffer. As shown in Fig. 1, the amount of PRC detected in untreated U2OS or T98G cells dropped precipitously upon dilution of the protease inhibitor mixture present in the cell lysis buffer. In contrast, the induced PRC expression detected in extracts prepared from cells treated with inhibitors of mitochondrial oxidative phosphorylation, either CCCP (Fig. 1*A*) or meclizine (Fig. 1*B*), was resistant to the progressive dilution of protease inhibitor. Interestingly, the expression of c-MYC followed a similar pattern. The low level of c-MYC expression detected in the absence of inducer was diminished upon dilution of the protease inhibitor mixture (Fig. 1). In con-

trast, the induced level of c-MYC expression by either CCCP (Fig. 1*A*) or meclizine (Fig. 1*B*) was protease-resistant. Thus, CCCP and meclizine act by inducing PRC and c-MYC protein expression and by conferring resistance of both proteins to *in vitro* proteolysis. The enhanced inducer-dependent proteolytic stability likely reflects a change in the physical state of these molecules that coincides with the activation of the stress program.

The tight coordinate response of PRC and c-MYC to multiple inducers of cellular stress (15, 16) raised the question of whether c-MYC is required for induction of the PRC-dependent stress response. This was tested using the small molecule MYC inhibitor 10058-F4, which inhibits c-MYC by blocking its heterodimerization with myc-associated factor X, resulting in diminished c-MYC levels (19). As shown in Fig. 2*A*, increasing concentrations of 10058-F4 inhibited the induction of both PRC and c-MYC by CCCP without affecting NRF-2α expression, demonstrating that c-MYC is required for the induction of PRC.

Treatment with c-MYC inhibitor also led to a concentration-dependent inhibition of the CCCP induction of representative PRC stress genes (*IL-1α, CCL20, ESM1,* and *CHRNA9*) (Fig.
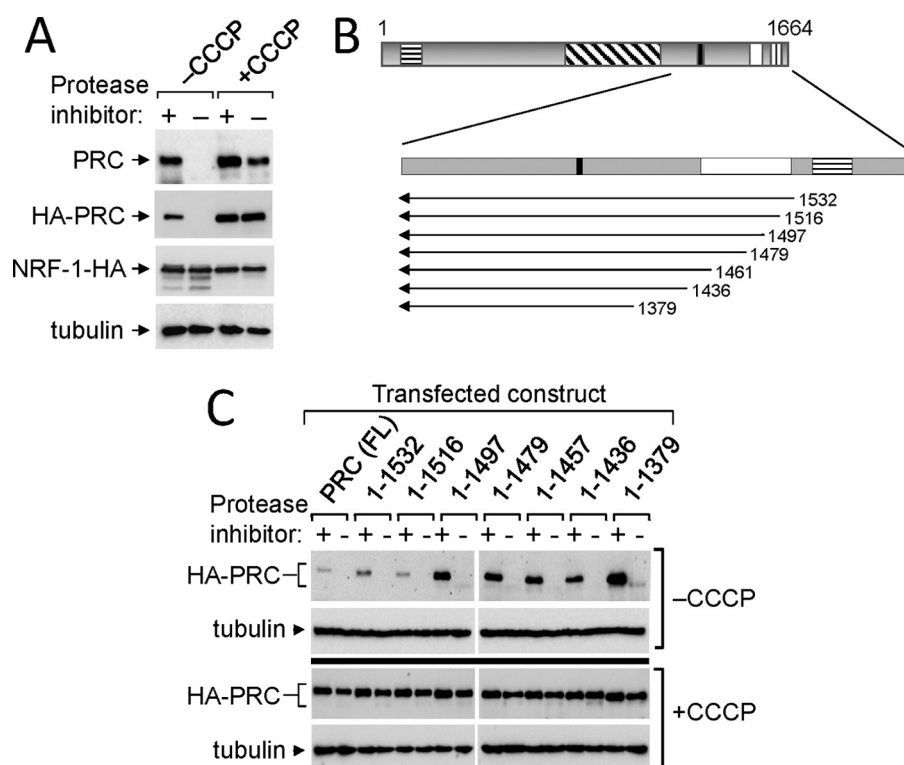
FIGURE 3. **Carboxyl-terminal deletion mapping of the PRC negative regulatory domain in PRC.** *A*, the response of endogenous PRC to CCCP induction and protease resistance was compared with that of HA-tagged PRC (HA-PRC) expressed from a transfected construct (HA-PRC/pSV-Sport). Controls included a cotransfected construct expressing NRF-1-HA and endogenous tubulin. Log phase U2OS cells were plated as in Fig. 1*A*, treated with either vehicle (−*CCCP*) or CCCP (+*CCCP*) and total cell extracts prepared in the presence (+) or the absence (−) of protease inhibitor mixture. Extracts were subjected to immunoblotting using rabbit anti-PRC(1047–1379), rat anti-HA, or mouse anti-tubulin antibodies. *B*, schematic representation of the PRC carboxyl-terminal deletion series. Positions of the activation domain (*horizontally striped box*), the proline-rich region (*hatched box*), the host cell factor binding site (*filled box*), the arginine/serine domain (*open box*), and the RNA recognition motif (*vertically striped box*) are indicated. *C*, the HA-tagged PRC derivative containing each carboxyl-terminal deletion depicted in *B* was constructed in HA-PRC/pSV-Sport and transfected into U2OS cells. Total cell extracts were prepared in the presence (+) or absence (−) of protease inhibitor mixture and subjected to immunoblotting using rat anti-HA or mouse anti-tubulin as the control. The same deletion series was analyzed from cells either untreated (−*CCCP*, *upper panels*) or treated with CCCP (+*CCCP*, *lower panels*).

2*B*). Although *PRC* and *Tfam* controls were also inhibited by 10058-F4, the effect was much greater for the PRC stress genes. At 100 μM 10058-F4, the induction of the PRC stress genes by CCCP was reduced significantly with little effect on the PRC and Tfam controls. At 200 μM 10058-F4, the induction of the stress genes by CCCP was inhibited 14−25-fold compared with 4−6-fold for *PRC* and *Tfam*. As observed previously (16), c-MYC mRNA was induced by CCCP, whereas PRC mRNA expression remained unchanged. c-MYC mRNA induction was also inhibited significantly at both 10058-F4 concentrations, suggesting that c-MYC and/or PRC is required for the stress-induced expression of c-MYC mRNA.

These results were confirmed by siRNA silencing of c-MYC. As shown in Fig. 2*C*, efficient silencing of c-MYC expression coincided with a marked reduction in PRC protein expression. The CCCP-induced level of PRC observed upon c-MYC silencing was below the uninduced level detected in cells treated with the control siRNA. Thus, both the pharmacological inhibition of c-MYC by 10058-F4 and c-MYC siRNA silencing are consistent with a requirement for c-MYC for the induction of PRC and the PRC stress genes by CCCP.

Identification of a PRC Negative Regulatory Domain Comprised of Tandem GSK-3 Consensus Phosphorylation Sites— Our current (Fig. 2*B*) and previous observations that the induction of PRC protein expression by CCCP was not accompanied

by a concomitant increase in PRC mRNA suggested that PRC induction occurred by a post-transcriptional mechanism (16). As a prelude to identifying the molecular determinants responsible, it was important to demonstrate that that PRC expressed from a transfected plasmid exhibited the same response to inducer as the endogenous protein. As shown in Fig. 3*A*, both endogenous PRC and HA-tagged PRC expressed from a transfected plasmid were induced by CCCP, and both exhibited inducer-dependent resistance to proteolysis. The controls included NRF-1-HA expressed from a transfected plasmid and endogenous tubulin, neither of which were induced by CCCP or affected significantly by the absence of protease inhibitor. Thus, HA-tagged PRC exhibited both the CCCP-dependent induction and protease resistance observed for the endogenous protein.

We had observed that a carboxyl-terminal deletion to PRC amino acid residue 1379 led to a marked increase in PRC steady-state expression, suggesting that the carboxyl-terminal domain contains a negative regulatory motif. Thus, a series of carboxyl-terminal deletions was constructed for the purpose of defining the negative regulatory domain within this region. As shown in Fig. 3 (*B* and *C*), progressive deletion from the carboxyl terminus led to increased PRC steady-state expression under conditions where the tubulin control was unaffected. Expression increased upon deletion of the interval between
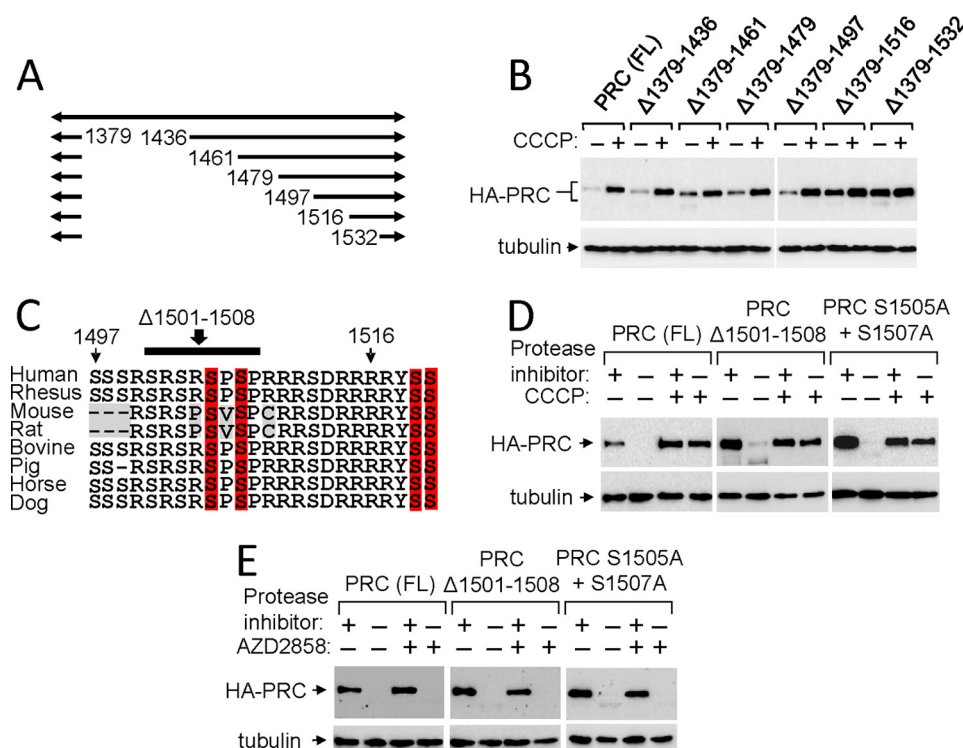
FIGURE 4. **Assignment of a negative regulatory motif to tandem GSK-3 consensus phosphorylation sites.** *A*, schematic representation of constructs used for deletion mapping. *B*, the deletion constructs described in *A* were analyzed for CCCP induction by immunoblotting following transfection as described in Fig. 1*B*. *C*, sequence comparison of the *PPRC1* gene from the indicated eight mammalian species in the region bounded by human PRC amino acids 1497–1520. The conserved GSK-3 consensus phosphorylation sites between amino acids 1501 and 1508 are indicated by a *solid bar*. Potential GSK-3 and Akt serine phosphorylation sites are shaded in *red*. *D*, the CCCP induction and protease resistance of HA-tagged full-length PRC was compared with that of the same construct containing either a small deletion encompassing the GSK-3 sites (PRCΔ1501–1508) or site-directed conversion of the serine phosphorylation sites at residues 1505 and 1507 to alanines (PRC S1505A+S1507A). *E*, the AZD2858 induction and protease resistance of HA-tagged full-length PRC was compared with that of the same construct containing either a small deletion encompassing the GSK-3 sites (PRCΔ1501–1508) or site-directed conversion of the serine phosphorylation sites at residues 1505 and 1507 to alanines (PRC S1505A+S1507A).

1516 and 1497 and remained high through deletion to residue 1379. Interestingly, all of the deleted molecules were completely degraded when the protease inhibitor mixture was omitted from the lysis buffer (Fig. 3*C*, −*CCCP, upper panels*). Thus, the carboxyl terminus has a marked effect on PRC steady-state expression without affecting its proteolytic stability.

When the same experiment was performed in cells treated with CCCP (Fig. 3*C*, +*CCCP, lower panels*), all of the deletion constructs were expressed at similar high levels relative to the tubulin control, and all were resistant to *in vitro* proteolysis in the absence of protease inhibitor. The findings suggest that treatment of cells with the inducer results in an intrinsic change in structure, a molecular interaction, or both, which enhances PRC stability *in vitro*. Notably, the induction of PRC by CCCP was diminished upon deletion of the interval between 1516 and 1497, which corresponded to the breakpoint for the enhanced steady-state expression in the absence of CCCP (Fig. 3*C*). Thus, the carboxyl-terminal domain bounded by amino acids 1664 and 1497 can act as a potent negative regulator of PRC steady-state levels.

The identification of the carboxyl terminus as a regulatory domain contributing to PRC induction was investigated further by constructing a series of progressive internal deletions from residues 1379 to 1532 (Fig. 4*A*) and testing the induction of each by CCCP (Fig. 4*B*). In agreement with the results of Fig. 3*C*, PRC induction was relatively unaffected until deletion of the interval bounded by residues 1497 and 1532 (Fig. 4*B*). This region contained perfect matches to GSK-3 ((S/T)XXX(S/T)P) (20) and Akt (RXRXX(S/T)) (21) consensus phosphorylation sites that are conserved among eight mammalian species (Fig. 4*C*). The suppression of PRC induction occurred in part because of the increased level of PRC expression in the absence of inducer, consistent with the deletion of a negative regulatory site.

GSK-3β can exert negative control of c-MYC expression through its phosphorylation of a GSK-3 site at Thr[58] (22, 23). The tight coordinate regulation of PRC and c-MYC suggested that PRC and c-MYC may be coordinately regulated by GSK-3. Therefore, the effect of GSK-3 on PRC induction was tested by introducing a small deletion removing the GSK-3 consensus sites at amino acid residues 1505 and 1507 (Fig. 4*C*, PRCΔ1501–1508). This small deletion led to high steady-state expression compared with full-length PRC and the loss of induction by CCCP (Fig. 4*D*). The result is consistent with the negative regulation of PRC expression through GSK-3 phosphorylation of one or both of these sites.

The role of GSK-3 was further confirmed by converting the two GSK-3 serine phosphorylation sites at amino acid residues 1505 and 1507 to alanines (PRC S1505A,S1507A). Interestingly, site-directed mutagenesis of these two residues alone resulted in an increase in PRC steady-state expression in the absence of inducer resembling that observed for the 1501–1508 deletion (Fig. 4*D*). These results strongly implicate the serine residues at

§ASBMB

1505 and/or 1507 as the sites of negative regulation by GSK-3. As with full-length PRC, the protease resistance of PRC(Δ1501–1508) and PRC(S1505A,S1507A) was dependent on the induction of cellular stress by CCCP (Fig. 4D). Thus, in the absence of inducer, GSK-3 acts as a negative regulator of PRC steady-state expression.

Further proof that GSK-3 acts through the GSK-3 sites bounded by PRC(Δ1501–1508) was obtained using AZD2858, a novel GSK-3 inhibitor developed by AstraZeneca (24). As observed with CCCP, AZD2858 induced PRC(FL) (Fig. 4E), a result consistent with the negative control of PRC expression by GSK-3. By contrast, the drug had no effect on the steady-state expression of PRC(Δ1501–1508) and PRC(S1505A,S1507A), confirming that the serine residues at 1505 and/or 1507 are required for negative regulation by GSK-3. Interestingly, in contrast with CCCP, AZD2858 induction of PRC was not accompanied by enhanced proteolytic stability. This is consistent with the results in Fig. 3C and suggests that CCCP-dependent step(s) are required for protease resistance.

Effects of GSK-3 Inhibition on the PRC Stress Program—If GSK-3 is a negative coordinate regulator of PRC and c-MYC expression, then GSK-3 inhibition would be expected to induce the endogenous proteins. As shown in Fig. 5A, treatment of cells with AZD2858 led to the induction of both PRC and c-MYC under conditions where the NRF-2α control was unaffected. However, compared with CCCP, AZD2858 was a less potent inducer of c-MYC induction under conditions where PRC displayed similar levels of induction by both agents. Drug concentrations were chosen based on their maximal induction of PRC protein levels, which occurred between 1 and 2 μM AZD2858 and 25 and 40 μM CCCP. Interestingly, CCCP treatment led to a robust increase in the phosphor-inactivated form of GSK-3β without changing the expression of either GSK-3α or β isoforms. By contrast, AZD2858 decreased both GSK-3α and β expression. Note that although the antibody used to detect phosphorylated GSK-3 is directed at both GSK-3α phosphorylation at Ser[9] and GSK-3β phosphorylation at Ser[21], all of the phosphor-GSK-3 detected comigrates with the β isoform. Thus, the CCCP induction of PRC and c-MYC coincides with an increase in the inactivated phosphorylated form of GSK-3β.

The induction of PRC and c-MYC by GSK-3 inhibition did not lead to the stabilization of either molecule to *in vitro* proteolysis (Fig. 5B). This result is consistent with the protease sensitivity observed for PRC(Δ1501–1508) and PRC(S1505A,S1507A) lacking the GSK-3 consensus sites (Fig. 4, D and E). Thus, blocking the phosphorylation of PRC by mutation of the GSK-3 sites or by inhibiting GSK-3 activity was not sufficient to confer protease resistance on either PRC or c-MYC.

A comparison of the induction of representative PRC stress genes (*IL-1α*, *CCL20*, *ESM1*, and *CHRNA9*) by CCCP to that of AZD2858 revealed a more modest induction by the GSK-3 inhibitor. In contrast to the robust induction of all four stress genes by CCCP (Fig. 5C), only two of the four (*IL-1α* and *ESM1*) were induced by AZD2858 (Fig. 5D) and at levels lower than that observed for CCCP (Fig. 5C). Thus, although both AZD2858 and CCCP led to the coordinate induction of PRC and c-MYC, the two agents exhibited quantitative differences
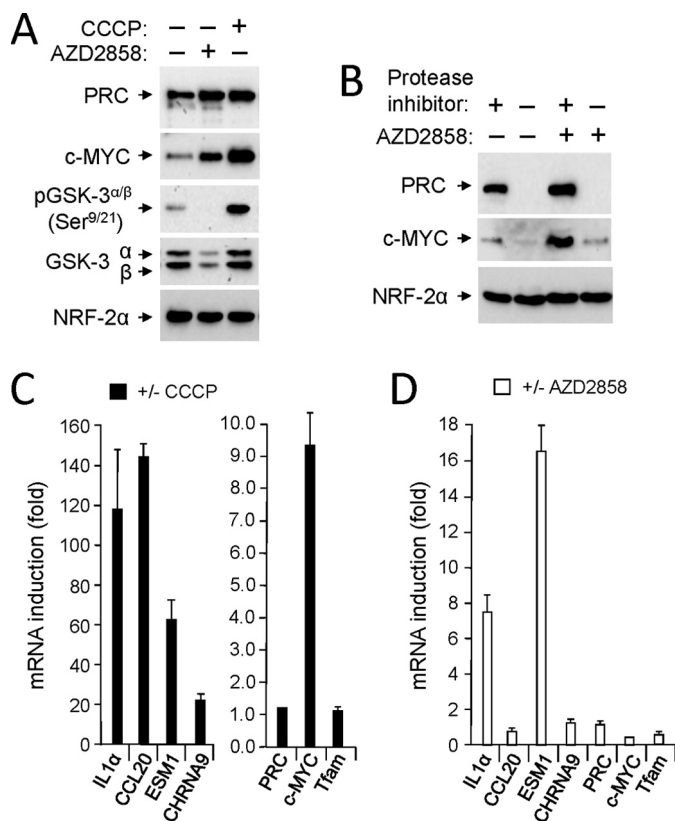

FIGURE 5. **Induction of the PRC stress program by GSK-3 inhibition.** *A*, human log phase U2OS cells were plated as in Fig. 1A and treated with either vehicle, the GSK-3 inhibitor, AZD2858, or CCCP for 24 h. Total cell extracts were subjected to immunoblotting using rabbit anti-PRC(1047–1379), mouse anti-c-MYC, rabbit anti-pGSK-3α/β(Ser[9/21]), rabbit anti-GSK-3α/β, or rabbit anti-NRF-2α as the control. *B*, U2OS cells were either untreated or treated with AZD2858. Total cell extracts were prepared in the presence (+) or absence (−) of protease inhibitor mixture and subjected to immunoblotting as in *A*. *C*, the fold induction by CCCP of the PRC stress genes (*IL1α*, *CCL20*, *ESM1*, and *CHRNA9*) compared with that of *PRC*, *Tfam*, and *c-MYC* was determined by quantitative real time PCR. *D*, The fold induction by AZD2858 of the PRC stress genes (*IL1α*, *CCL20*, *ESM1*, and *CHRNA9*) compared with that of *PRC*, *Tfam*, and *c-MYC* was determined by quantitative real time PCR. For *C* and *D*, RNA induction for each gene is expressed relative to the untreated control. The values are the averages ± S.E. for at least three independent experiments with a minimum of two technical replicas for each determination.

in their effects on stress gene expression. These differences, along with the inability of AZD2858 to confer protease resistance on either PRC or c-MYC, suggest that stress-dependent events, in addition to the induction of PRC and c-MYC proteins by GSK-3 inhibition, are required for maximal activation of the PRC stress program. The results are consistent with the c-MYC inhibitor experiments (Fig. 2) and further confirm that c-MYC is limiting for maximal induction of the PRC stress program.

As observed for other inducers of the program (16), neither Tfam nor PRC mRNAs were induced significantly by either CCCP or AZD2858. This contrasts with c-MYC mRNA, which was induced ~9-fold by CCCP (Fig. 5C) but not at all by AZD2858 (Fig. 5D). The inability of AZD2858 to induce c-MYC mRNA coincided with the muted induction of c-MYC protein and of the PRC stress genes (Fig. 5). The results suggested that in contrast to PRC, control of c-MYC expression at the mRNA level is a major contributor to the stress response.

Because c-MYC is known to be regulated both transcriptionally and post-transcriptionally, it was of interest to assess the
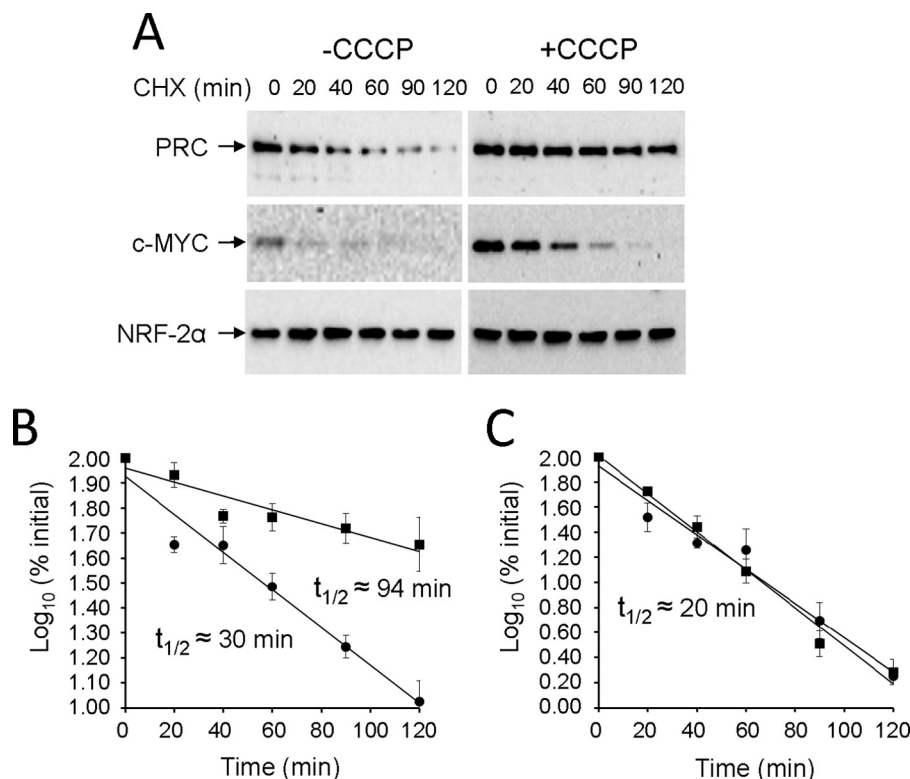
FIGURE 6. **PRC and c-MYC protein half-lives in CCCP-treated and untreated cells.** Human log phase U2OS cells were plated in 6-well plates and 24 h later were treated with either vehicle or CCCP for 16 h. The cells were then treated with cycloheximide at 40 μg/ml and harvested at 0, 20, 40, 60, 90, and 120 min following cycloheximide treatment. Whole cell extracts were prepared and subjected to immunoblotting using rabbit anti-PRC(1047–1379), mouse anti-c-MYC, or rabbit anti-NRF-2α antibodies. *A*, representative immunoblot showing the decay of PRC, c-MYC, and NRF-2α proteins following cycloheximide treatment of either vehicle- (−*CCCP*) or CCCP-treated (+*CCCP*) cells. *B*, time course of PRC protein decay in untreated (*filled circles*) or CCCP-treated (*filled squares*) cells as a function of the Log$_{10}$ of the percent of the initial PRC expression level at time 0 min normalized to the NRF-2α control. *C*, time course of c-MYC protein decay in untreated (*filled circles*) or CCCP-treated (*filled squares*) cells as a function of the Log$_{10}$ of the percentage of the initial c-MYC expression level at time 0 min normalized to the NRF-2α control. Half-lives were determined as the Log$_{10}$ of 50% extrapolated from the best fit linear decay line for each condition. Each point represents the average ± S.E. for five independent experiments.

contribution of changes in protein half-life to the CCCP-induced expression of both proteins. This was accomplished by measuring the rate of protein decay following treatment of cells with cycloheximide. As shown in Fig. 6, in untreated cells, PRC and c-MYC exhibited short protein half-lives of ~30 min (Fig. 6*B*) and 20 min (Fig. 6*C*), respectively. However, in CCCP-treated cells, the PRC half-life increased severalfold to ~94 min (Fig. 6*B*), whereas the c-MYC half-life remained relatively unchanged (Fig. 6*C*). This result, in conjunction with the differences in mRNA induction, suggested that PRC induction is regulated post-translationally. The increased PRC half-life by CCCP is consistent with the mutational analyses showing enhanced PRC steady-state expression upon mutation of the GSK-3 consensus phosphorylation sites (Fig. 4).

Akt-GSK-3β Signaling in the Response to Respiratory Chain Uncoupler—In confirmation of the data in Fig. 5*A*, the coordinate induction of PRC and c-MYC by CCCP was accompanied by an increase in the phosphor-inactivated form of GSK-3β without affecting total GSK-3α or β (Fig. 7*A*). Moreover, the induction of PRC, c-MYC, and GSK-3β by CCCP coincided with an increase in Akt activation as measured using an antibody specific to the activated form of Akt phosphorylated at Ser^{473} (pAkt(Ser^{473})) (Fig. 7*A*). This is consistent with the findings of others showing Akt activation in response to mitochondrial stress (25). The effect of Akt activation on the CCCP

induction of PRC and c-MYC was tested using the Akt inhibitor MK-2206, which inhibits Ser^{473} phosphorylation and activation of Akt (26). Akt activation was completely blocked when MK-2206 was included in the culture medium (Fig. 7*A*). The suppression of Akt activation by MK-2206 occurred in the absence of a similar reduction of total Akt levels and coincided with the down-regulation of PRC, c-MYC, and the phosphor-inactivated from of GSK-3β (Fig. 7*A*). Thus, activated Akt is a positive regulator of PRC and c-MYC induction by CCCP.

The role of Akt activation on the induction of the PRC stress genes was determined by measuring the inhibitory effect of MK-2206 on PRC stress gene induction by CCCP. As shown in Fig. 7*B*, the induction of the PRC stress genes (*IL-1α*, *CCL20*, and *ESM1*) by CCCP was markedly inhibited by MK-2206 compared with a modest inhibition of the *PRC* and *TFAM* controls. Note that the inhibition of the CCCP-induced expression of *CHRNA9* by MK-2206 fell just outside the range of statistical significance with a *p* value of 0.09. The coordinate down-regulation of PRC stress gene induction by the Akt inhibitor argues that an Akt-dependent step is required for activation of the PRC stress program by CCCP. This likely involves the phosphor-inactivation of GSK-3β by Akt. The results are consistent with a role for Akt-GSK-3 stress signaling for the concerted action of PRC and c-MYC in the induction of the PRC stress response to respiratory chain uncoupler.
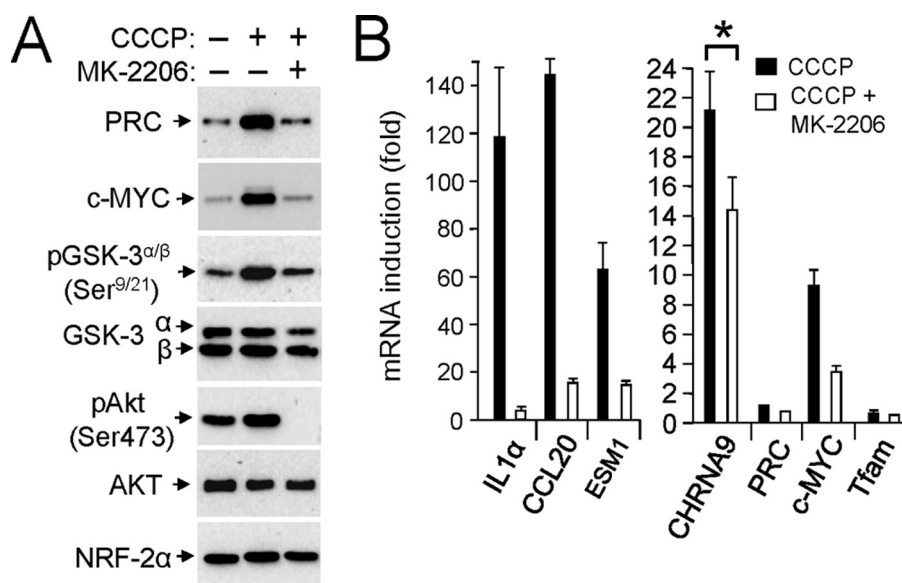
FIGURE 7. **Effect of GSK-3 and Akt signaling on the induction of the PRC stress program by CCCP.** *A*, cells plated as in Fig. 1*A* were treated with vehicle or CCCP in the absence or presence of the Akt inhibitor, MK-2206. Total cell extracts were prepared and subjected to immunoblotting using rabbit anti-PRC(1047–1379), mouse anti-c-MYC, rabbit anti-pGSK-3α/β (Ser$^{9/21}$), rabbit anti-GSK-3α/β, rabbit anti-pAkt (Ser^{473}), rabbit anti-Akt, or rabbit anti-NRF-2α antibodies. *B*, the fold induction by CCCP alone or CCCP plus MK-2206 of the PRC stress genes (*IL1α*, *CCL20*, *ESM1*, and *CHRNA9*) was compared with that of *PRC*, *Tfam*, and *c-MYC* by quantitative real time PCR. RNA induction for each gene is expressed relative to the untreated control. The values are the averages ± S.E. for at least three independent experiments with a minimum of two technical replicas for each determination. Differences with a *p* value of >0.05 were taken as statistically insignificant as indicated by *asterisk*.

Inducer Specificity of the PRC Stress Response—It was of interest to determine whether Akt-GSK-3 signaling was a general feature of the PRC- and c-MYC-dependent response to mitochondrial impairment. Meclizine is an inhibitor of mitochondrial respiration that induces PRC and c-MYC coordinately along with several of the PRC stress genes (16). Surprisingly, the coordinate induction of PRC and c-MYC by meclizine was not accompanied by increased phosphor-inactivated GSK-3β relative to total GSK-3 levels (Fig. 8*A*). However, Akt phosphorylation was induced by meclizine in the absence of an increase of total Akt. Moreover, the complete suppression of activated Akt by MK-2206 led to diminished PRC and c-MYC protein induction (Fig. 8*A*), although not to the baseline levels observed for CCCP (Fig. 7*A*). These results suggest that Akt may signal to PRC and c-MYC through a GSK-3-independent mechanism.

Although meclizine induced the expression of all four representative PRC stress genes, the magnitude of the response for several of the genes (*CCL20*, *ESM1*, and *CHRNA9*) was lower compared with that mediated by CCCP (Fig. 8*C*). However, meclizine induced IL-1α mRNA to a level comparable with that mediated by CCCP, and its induction was inhibited significantly by MK-2206. Thus, the Akt-dependent induction of *IL-1α* is common to both inhibitors of mitochondrial energy production. This is notable because of the central role of IL-1α in stress signaling (27, 28). By contrast, *CCL20* was not affected significantly by MK-2206, and *ESM1* and *CHRNA9* were markedly induced by the Akt inhibitor. Thus, although the induction of all four PRC stress genes is common to both inducers, Akt inhibition can exert inducer-specific effects on the expression of individual genes. The results suggest that inducer-specific signaling mechanisms operate to modulate the response to alternative forms of mitochondrial stress.

The differential effects of AZD2858, CCCP, and meclizine on the expression of the PRC stress genes may result from the severity of the stress elicited by each agent. Cells treated with AZD2858, under conditions of maximal PRC induction, were indistinguishable morphologically from untreated cells, were mitotically active (Fig. 9*A*), and exhibited little loss of cell viability (Fig. 9*B*). By contrast, CCCP- or meclizine-treated cells became growth-arrested with a significant loss of cell viability. The CCCP-treated cells exhibited numerous cytoplasmic projections, whereas the cytoplasm of meclizine-treated cells became extensively vacuolated (Fig. 9*A*). These features differ from the senescent phenotype observed for SN-38-treated cells (16) and confirm that the coordinate induction of PRC and c-MYC is independent of the morphological changes associated with individual stress inducers.

It was possible that variation in stress gene expression resulted from differences in the oxidant sensitivity of the response of PRC and c-MYC to each inducer. As observed previously, the PRC stress response to CCCP and menadione was blocked by NAC, whereas the response to SN-38 was NAC-resistant (16). As shown in Fig. 8*C*, the induction of PRC and c-MYC by all three agents was inhibited by NAC. Thus, differences in oxidant signaling are unlikely to account for the inducer-specific effects on stress gene expression. The results suggest that the stress response differed according to the severity of the effect of each agent on cell viability. Notably, diminished cell viability by meclizine and CCCP coincided with the enhanced proteolytic stability of both PRC and c-MYC, suggesting a contribution by stress-dependent factors related to growth arrest.

Discussion

Here, we show that c-MYC works in concert with PRC as an essential component of the PRC-dependent response to mito-
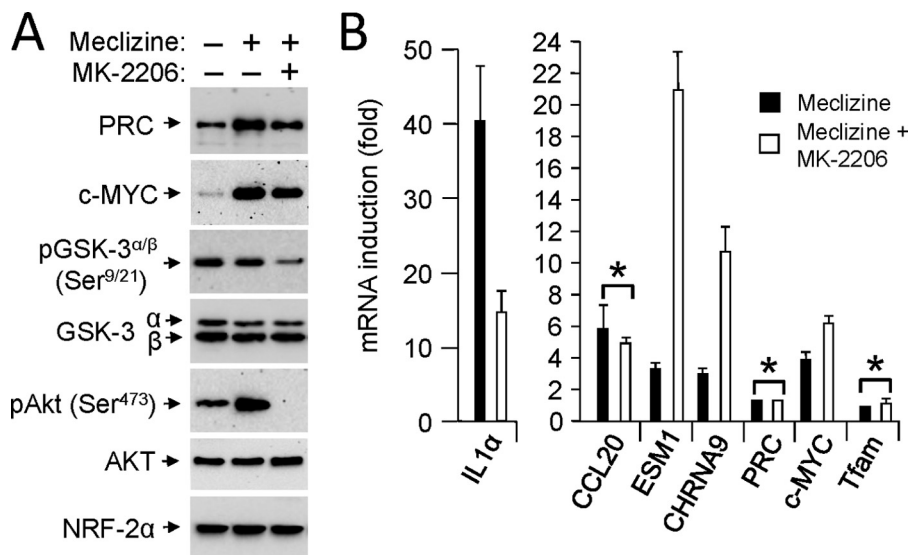
FIGURE 8. **Effect of GSK-3 and Akt signaling on the induction of the PRC stress program by meclizine.** *A*, cells plated as in Fig. 1*A* were treated with vehicle or meclizine in the absence or presence of the Akt inhibitor, MK-2206. Total cell extracts from subconfluent cells were prepared and subjected to immunoblotting using rabbit anti-PRC(1047–1379), mouse anti-c-MYC, rabbit anti-pGSK-3α/β (Ser$^{9/21}$), rabbit anti-GSK-3α/β, rabbit anti-pAkt (Ser^{473}), rabbit anti-Akt, or rabbit anti-NRF-2α antibodies. *B*, the fold induction by meclizine alone or meclizine plus MK-2206 of the PRC stress genes (*IL1α, CCL20, ESM1*, and *CHRNA9*) was compared with that of *PRC, Tfam*, and *c-MYC* by quantitative real time PCR. RNA induction for each gene is expressed relative to the untreated control. The values are the averages $\pm$ S.E. for three independent experiments with a minimum of two technical replicas for each determination. Differences with a *p* value of >0.05 were taken as statistically insignificant as indicated by *asterisk*.
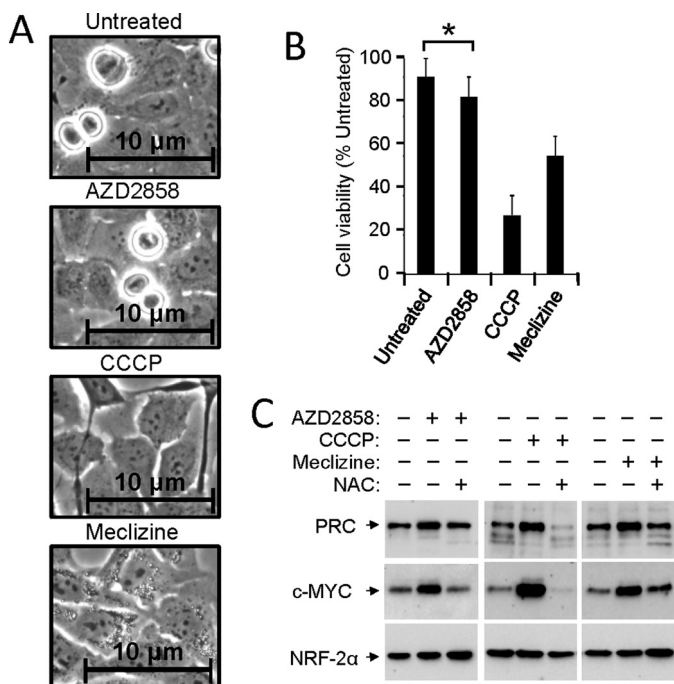
FIGURE 9. **Inducer specificity of the PRC stress response.** *A*, cells plated as in Fig. 1*A* were either left untreated or treated with AZD2858, CCCP, or meclizine under conditions of maximal PRC induction by each agent. The cells were visualized by phase contrast microscopy. *B*, viability of cells treated as in *A* was determined using a resazurin-based fluorescence assay. The values represent the average cell viability relative to the untreated control $\pm$ S.E. for three independent experiments with a minimum of two technical replicas for each determination. Differences with a *p* value >0.05 were taken as statistically insignificant as indicated by *asterisk*. *C*, the effect of NAC on the induction of PRC and c-MYC by AZD2858, CCCP, or meclizine was determined by immunoblotting using rabbit anti-PRC(1047–1379), mouse anti-c-MYC, or rabbit anti-NRF-2α as the control.

chondrial stress. Silencing of c-MYC by siRNA diminished PRC expression, and the c-MYC inhibitor 10058-F4 inhibited the induction of PRC, c-MYC, and representative PRC stress genes

by respiratory chain uncoupler. In addition, both PRC and c-MYC acquired protease resistance upon their induction by CCCP or meclizine in cells of markedly different tissue origins. This inducer-dependent protease resistance, assayed by the stability of both proteins upon dilution of protease inhibitor mixture in the cell lysis buffer, likely reflects an intrinsic change in the structure of these molecules that facilitates the reprogramming gene expression (Fig. 10).

However, this *in vitro* stability appears not to reflect a common intracellular mechanism of PRC and c-MYC turnover because CCCP treatment increased PRC half-life without affecting that of c-MYC. Notably, PRC has been identified as a member of the ubiquitin-modified proteome (29), and PRC expression is abundantly induced by proteasome inhibitors (15). Stress-inducible post-translational modifications that regulate the delivery of proteins to the proteasome through their effects on E3 ligases have been described (30).

GSK-3β is a known negative regulator of c-MYC expression through its phosphorylation of Thr^{58}, an event that promotes c-MYC degradation by the ubiquitin proteasome system (23, 31). GSK-3β inhibition by AZD2858 led to the robust induction of PRC consistent with the negative regulation of PRC through its phosphorylation by GSK-3β. However, failure of the GSK-3 inhibitor to induce c-MYC mRNA correlated with a more muted induction of both c-MYC protein and of the PRC stress genes. Thus, although PRC is necessary for the induction of the inflammatory stress program, it is not sufficient to trigger a robust response in the absence of a concomitant increase in c-MYC expression. The results support the conclusion that PRC and c-MYC induction by CCCP occurs through coordination of c-MYC mRNA expression with the post-translational induction of PRC.

In addition to the induction of PRC by GSK-3β inhibition, the negative regulation of PRC through GSK-3β phosphoryla-
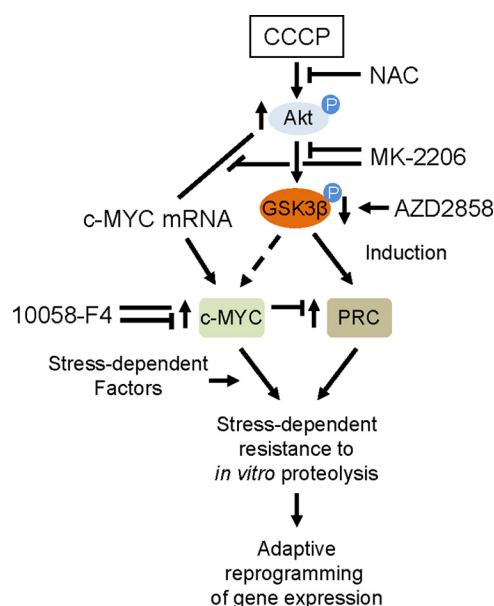
FIGURE 10. **Schematic representation of the pathway of mitochondrial stress signaling through CCCP.** Mitochondrial stress, resulting from the dissipation of the mitochondrial membrane potential by CCCP, leads to the activation of Akt, which can phosphor-inactivate GSK-3β. This relieves the negative control of PRC expression by inhibiting the phosphorylation of the GSK-3β consensus sites at PRC Ser$^{1505/1507}$, leading to a severalfold increase in PRC protein half-life. However, unlike PRC induction, which is exclusively post-translational, c-MYC induction occurs predominantly through a 9-fold increase in mRNA expression, with little change in the c-MYC protein half-life. Although PRC and c-MYC protein expression are both induced by the GSK-3 inhibitor, AZD2858, the effect on c-MYC and the PRC stress genes is muted (*dashed arrow*) compared with that achieved with CCCP. The pathway is blocked by the Akt inhibitor MK-2206 and by the antioxidant NAC, presumably because signaling to Akt is dependent on mitochondrial ROS. The c-MYC inhibitor 10058-F4 blocks the induction of c-MYC, PRC, and representative stress genes, demonstrating an essential requirement for c-MYC, an effect confirmed by c-MYC silencing. In addition to the induction of PRC and c-MYC, full execution of the stress response requires unidentified stress-dependent events that coincide with the *in vitro* protease resistance of both proteins. We speculate that this stress-dependent resistance to *in vitro* proteolysis reflects a change in the physical state of both that is required for the adaptive reprogramming of gene expression.

tion was further supported by mutational analyses. Following the identification of a negative regulatory domain by fine deletion mapping, conversion to alanines of GSK-3 consensus serine phosphorylation sites at amino acids 1505 and 1507 within this domain led to markedly elevated PRC protein levels. It is notable that these same PRC GSK-3 sites were identified as serine phosphorylation sites in the phosphoproteome of human embryonic stem cells (32). Moreover, PRC induction by CCCP was accompanied by a marked increase in the phosphor-inactivation of GSK-3β, a result consistent with the derepression of PRC induction through inhibition of its phosphorylation by GSK-3β. Thus, multiple independent lines of evidence support the regulatory role of GSK-3β in the post-translational control of PRC steady-state expression. We conclude that the down-regulation of GSK-3β is a terminal event in a stress signaling pathway that responds to respiratory chain uncoupling by up-regulating PRC (Fig. 10).

Akt is one of a number of stress kinases that can phosphorylate and thereby repress GSK-3 activity (33). The observation that the inhibition of Akt activation by MK-2206 blocks the CCCP induction of PRC, c-MYC, and the PRC stress genes

argues that CCCP requires Akt activation to orchestrate the stress response. In addition to its role in the phosphor-inactivation of GSK-3, Akt may be required for the expression of interacting partners, a modification of PRC or its cofactors, or some combination of the two. Others have shown that increased Akt activation is required for mitochondrial stress signaling through direct phosphorylation of the hnRNPA2 coactivator (25).

Although PRC and c-MYC protein expression are tightly coordinated in response to a number of stress inducers, only c-MYC is induced at the mRNA level by both CCCP and meclizine (16). AZD2858 differs from CCCP and meclizine in that it does not enhance the proteolytic stability of PRC and c-MYC and has no significant effect on cell viability. The results argue that stress-dependent events that impact cell viability are required for full execution of the stress program (Fig. 10). c-MYC mRNA induction has been observed in response to mitochondrial dysfunction resulting from depletion of mitochondrial DNA (34, 35). Although the specific function of c-MYC in retrograde (mitochondria to nucleus) signaling has not been investigated, the findings are consistent with the increased c-MYC mRNA and protein expression observed upon treatment of cells with multiple stress inducers, including mitochondrial inhibitors (16).

Although meclizine induction of the stress program requires PRC (16), its induction of PRC and c-MYC did not coincide with the increased phosphor-inactivation of GSK-3β. In contrast to CCCP, which acts directly to uncouple the respiratory chain, meclizine inhibits mitochondrial respiration through its inhibition of phosphoethanolamine metabolism (36). PRC is a large molecule with many potential modification sites, and it is likely that meclizine mediates its effects through unidentified stress-dependent modifications. The differential effects of Akt inhibition on the meclizine induction of several PRC stress genes may reflect alternative regulatory inputs.

Despite these differences, IL-1α mRNA is markedly induced by both CCCP and meclizine, and in both cases its induction is inhibited by the Akt inhibitor MK-2206. The results suggest that Akt-dependent induction of IL-1α is common to mitochondrial stress pathways. The interleukin-1 family of cytokines exerts pleiotropic effects including the induction of a large number of genes in many cell types (37). Although the extracellular effects of IL-1 in inflammation are well established, much less is known about its intracellular actions (38). IL-1α plays a major role in sterile inflammation (39) and is a sensor of DNA damage (27). It is also a major driver of the senescence-associated inflammation that has been linked to age-related disease (28, 40). The PRC- and c-MYC-dependent induction of IL-1α in response to mitochondrial stress may represent a novel link between mitochondrial dysfunction and age-related inflammation.

A number of studies have linked c-MYC to stress response programs that are adaptive in promoting cell survival (reviewed in Ref. 41). Functional roles for c-MYC include the induction of autophagy (42, 43), activation of the DNA damage response (44), promotion of a pro-survival antioxidant response (45), and the generation of an inflammatory program that facilitates

tumor progression (46). In the latter case, MYC has been implicated in tumor angiogenesis through the pro-inflammatory cytokine, IL-1β, providing a link between MYC-driven inflammation and the remodeling of the tumor microenvironment (47). Moreover, a recent gain-of-function screen for human proteins that control mitochondrial function identified *GLTSCR2/PICT1* as an evolutionarily conserved regulator of mitochondrial respiration (48). Interestingly, *GLTSCR2* was found to regulate MYC expression, and both were up-regulated in response to mitochondrial stress. The results implicated *GLTSCR2* and MYC in the adaptive response to mitochondrial impairment. These examples are consistent with a role for MYC in linking mitochondrial dysfunction to pro-survival stress pathways.

The concerted action of PRC and c-MYC in reprogramming gene expression in response to mitochondrial stress represents a novel functional association. The control of c-MYC expression through Akt-GSK-3 signaling has been documented (22, 23), and the current findings implicate a similar pathway in the control of PRC expression in response to CCCP. Both proteins are up-regulated in human cancers (13, 49) where aerobic glycolysis contributes essential intermediates for rapid proliferation (50) and where a pro-inflammatory microenvironment can promote tumor progression (51). Concerted action by PRC and c-MYC may contribute to these through increased lactate production and the induction of inflammatory and glycolytic gene expression (15, 16). This is consistent with recent findings linking c-MYC to inflammatory mediators that promote tumor progression (46, 47).

The discovery of a pro-survival inflammatory stress program mediated through the concerted action of PRC and c-MYC may provide insights for targeting pro-survival pathways in the context of human disease. Akt is encoded by an oncogene that is up-regulated in human cancers (52) and has been implicated in the inactivation of the apoptotic machinery (53, 54), making it an important therapeutic target. The Akt inhibitor, MK-2206, which inhibits the PRC stress response to CCCP, is currently in clinical trials (55, 56). In addition, GSK-3 inhibition by AZD2858 has been associated with enhanced osteogenesis in rodent models (24). However, signaling through Akt and GSK-3 can affect many essential cellular functions including cell proliferation and metabolism (33, 57). Thus, it may be desirable to target only those adaptive functions that promote cell survival. Further understanding of the molecular mechanisms driving the PRC and c-MYC response to mitochondrial stress may lead to new targets that can modulate the pro-survival machinery, leading to more effective therapeutics.

Experimental Procedures

Plasmids—The amino-terminal HA tag in the plasmid HA-FL-PRC/pSV-Sport was derived by incorporating an HA tag-containing SalI/AscI fragment derived from pSG5NRF-1-HA (58) by PCR using sense (5′-AAAGTCGACTGGGTGTTCAG-GGGCCAAGATGTATCCTTATGATGTTCCT-3′) and antisense (5′-AAAGGCGCGCCGCAGCGTAATCAGGAACAT-CATAAGGATA-3′) primers. The PRC amino terminus in

FL-PRC/pSV Sport (14) was replaced with the SalI/AscI PCR product containing the HA tag.

PRC carboxyl-terminal deletions (residues 1–1532, 1–1516, 1–1497, 1–1479, 1–1461, 1–1436) were generated by PCR using HA-FL-PRC/pSV-Sport as a template. PRC fragments containing the deletions were amplified using a DraIII sense primer (5′-AAAAAACACAAGGTGTCTGCCCTGGTGCA-3′) and the corresponding NotI antisense deletion primers (1–1532, 5′-AAAAGCGGCCGCTCACACTCTTTGCC-TTTGG-3′; 1–1516, 5′-AAAAGCGGCCGCTCACCGCCTC-CTGTCACT-3′; 1–1497, 5′-AAAAGCGGCCGCTCAGGA-TGATGAGGATGA-3′; 1–1479, 5′-AAAAGCGGCCG-CTCAGCATCTTCGAGAACG-3′; 1–1457, 5′-AAAAGCG-GCCGCTCAGGACCTGGACCGAGA-3′; AND 1–1436, 5′-AAAAGCGGCCGCTCACCGGTTGGACCCAGA-3′). The carboxyl-terminal DraIII-NotI fragment of HA-FL-PRC/pSV Sport was replaced by the individual PCR products containing the deletion. HA-PRC(1–1379)/pSV-Sport was derived from PRC(1–1379)/pSV-Sport (3).

Internal PRC deletions (Δ1379–1436, Δ1379–1461, Δ1379–1479, Δ1379–1497, Δ1379–1516, Δ1379–1532, and Δ1501–1508) and site-directed point mutations (S1505A,S1507A) were introduced by PCR using HA-FL-PRC/pSV-Sport as a template as described (3). PCR primers containing the desired base changes or deletions were used in conjunction with either the DraIII-containing sense or NotI-containing antisense primers used for the carboxyl-terminal deletions to generate overlapping PCR products that were then used as templates for the amplification of a DraIII-NotI PCR product for cloning into DraIII and NotI-digested HA-FL-PRC/pSV-Sport. The mutagenesis primers were as follows: Δ1379–1436 (sense 5′-TTGCTGTCCCCTGAGACTAGCGAAGCA-TCT-3′ and antisense 5′-AGATGCTTCGCTAGTCTC-AGGGGACAGCAA-3′), Δ1379–1461 (sense 5′-TTGCT-GTCCCCTGAGCACAAGAGGTGGCGA-3′ and antisense 5′-TCGCCACCTCTTGTGCTCAGGGGACAGCAA-3′), Δ1379–1479 (sense 5′-TTGCTGTCCCCTGAGTCTT-CCTCTTCTTCG-3′ and antisense 5′-CGAAGAAGAG-GAAGACTCAGGGGACAGCAA-3′), Δ1379–1497 (sense 5′-TTGCTGTCCCCTGAGAGTTCTCGAAGCCGC-3′ and antisense 5′-GCGGCTTCGAGAACTCTCAGGGGACAG-CAA-3′), Δ1379–1516 (sense 5′-TTGCTGTCCCCTGAGC-GGTACAGCTCTTAT-3′ and antisense 5′-ATAAGAGCT-GTACCGCTCAGGGGACAGCAA-3′), Δ1379–1532 (sense 5′-TTGCTGTCCCCTGAGCTACAAAAGGAGCGT-3′ and antisense 5′-ACGCTCCTTTTGTAGCTCAGGGGACA-GCTT-3′), Δ1501–1508 (sense 5′-TCATCATCCAGT-TCTCGACGCCGGAGAAGTGACAGG-3′ and antisense 5′-CCTGTCACTTCTCCGGCGTCGAGAACTGGATGATGA-3′), and S1505A,S1507A (sense 5′-AGCCGCTCACGA*G*CAC-CA*G*CACCCCGCCGGAGA-3′ and antisense 5′-TCTCC-GGCGGGG*T*GCTGG*T*GCTCGTGAGCGGCT-3′).

Cell Culture and Transfections—U2OS and T98G cells were obtained from ATCC and maintained in DMEM (Invitrogen) with 10% fetal bovine serum (HyClone) and 1% penicillin-streptomycin (Invitrogen). The cells were plated at a density of 1×10^6 cells/10-cm dish, grown for 24–48 h, and then subjected to treatment with various agents as follows: 40 μM

CCCP (Sigma), 50–200 μM 10058-F4 (Sigma), 1–2 μM AZD2858 (MedChem Express), and 10 μM MK-2206 (a gift from J. Julie Kim, Department of Obstetrics and Gynecology, Northwestern Medical School) in DMSO. Vehicle controls were treated with either DMSO or H_2O as appropriate.

siRNA—Silencing of c-MYC protein expression in U2OS cells was achieved using ON-TARGETplus Human MYC siRNA SMARTpool with ON-TARGETplus non-targeting pool as a negative control (GE Healthcare Dharmacon, Inc.). The cells were plated in 6-well plates at a density of 1.9×10^5 cells/well and transfected with 100 nM siRNA using Lipofectamine 2000 (Invitrogen). At 48 h post-transfection, the cells were treated with 40 μM CCCP or vehicle control for 16 h, and the cell extracts were prepared for immunoblotting.

Immunoblotting—Whole cell lysates were prepared in Nonidet P-40 lysis buffer as described previously (14). A 7$\times$ stock solution of protease inhibitor was prepared by dissolving one tablet of Complete Mini protease inhibitor mixture (Roche) in 1.2 ml of H_2O. Unless otherwise indicated, protease inhibitor was used at a concentration of 1$\times$ in the cell lysis buffer. Extracts were subjected to denaturing gel electrophoresis, and the proteins were transferred to nitrocellulose membranes (Schleicher & Schuell) as described (7, 15). Primary antibodies were rabbit anti-PRC (1047–1379) (3), mouse anti-c-Myc (9E10) (Thermo Scientific), rabbit anti-NRF2α (59), mouse anti-tubulin (Sigma), rabbit anti-pGSK-3α/β (Ser$^{9/21}$) (Cell Signaling), rabbit anti-GSK-3α/β (Cell Signaling), rabbit anti-pAkt (Ser^{473}) (Cell Signaling), and rabbit anti-Akt (Cell Signaling). Hemagglutinin-tagged proteins were detected using rat anti-HA-peroxidase monoclonal antibody (Roche).

Quantitative Real Time PCR—Total RNA was purified using TRIzol reagent (Invitrogen) and quantitative real time PCR carried out as described (7, 15, 16).

Protein Half-life Determination—Human log phase U2OS cells were plated in 6-well plates at a cell density of $3-4 \times 10^5$ cells/well and 24 h later were treated with either vehicle ($-$) or CCCP ($+$) for 16 h. The cells were then treated with cycloheximide (40 μg/ml; Sigma) and harvested at various times following cycloheximide treatment. Whole cell extracts were prepared and subjected to immunoblotting using rabbit anti-PRC(1047–1379), mouse anti-c-MYC, or rabbit anti-NRF-2α antibodies. Immunoblots were imaged, and protein bands were quantitated using a Bio-Rad ChemiDoc XRS+ with Image Lab software. The values were normalized to the NRF-2α control for each time point, and the protein degradation rate ($t_{1/2}$) is expressed as the time for degradation of 50% of the protein.

Cell Viability Assay—U2OS cells were plated at 20,000 cells/well in a black-walled 96-well plate and allowed to grow for 24 h. The cells were treated with AZD2858 (24 h), CCCP (24 h), or meclizine (72 h), washed twice with PBS, and treated with medium containing 10 μg/ml resazurin (Sigma) for 1.5 h. Fluorescence was measured in a Spectramax fluorescence microplate reader with an excitation and emission wavelengths of 545 and 590 nm, respectively.

References

1. Scarpulla, R. C. (2011) Metabolic control of mitochondrial biogenesis through the PGC-1 family regulatory network. *Biochim. Biophys. Acta* **1813,** 1269–1278
2. Scarpulla, R. C., Vega, R. B., and Kelly, D. P. (2012) Transcriptional integration of mitochondrial biogenesis. *Trends Endocrinol. Metab.* **23,** 459–466
3. Vercauteren, K., Pasko, R. A., Gleyzer, N., Marino, V. M., and Scarpulla, R. C. (2006) PGC-1-related coactivator: immediate early expression and characterization of a CREB/NRF-1 binding domain associated with cytochrome c promoter occupancy and respiratory growth. *Mol. Cell Biol.* **26,** 7409–7419
4. Herschman, H. R. (1991) Primary response genes induced by growth factors and tumor promoters. *Annu. Rev. Biochem.* **60,** 281–319
5. Winkles, J. A. (1998) Serum- and polypeptide growth factor-inducible gene expression in mouse fibroblasts. *Prog. Nucleic Acids Res. Mol. Biol.* **58,** 41–78
6. Fowler, T., Sen, R., and Roy, A. L. (2011) Regulation of primary response genes. *Mol. Cell* **44,** 348–360
7. Vercauteren, K., Gleyzer, N., and Scarpulla, R. C. (2009) Short hairpin RNA-mediated silencing of PRC (PGC-1-related coactivator) results in a severe respiratory chain deficiency associated with the proliferation of aberrant mitochondria. *J. Biol. Chem.* **284,** 2307–2319
8. Larsson, N. G., Wang, J., Wilhelmsson, H., Oldfors, A., Rustin, P., Lewandoski, M., Barsh, G. S., and Clayton, D. A. (1998) Mitochondrial transcription factor A is necessary for mtDNA maintenance and embryogenesis in mice. *Nat. Genet.* **18,** 231–236
9. Park, C. B., Asin-Cayuela, J., Cámara, Y., Shi, Y., Pellegrini, M., Gaspari, M., Wibom, R., Hultenby, K., Erdjument-Bromage, H., Tempst, P., Falkenberg, M., Gustafsson, C. M., and Larsson, N. G. (2007) MTERF3 is a negative regulator of mammalian mtDNA transcription. *Cell* **130,** 273–285
10. Metodiev, M. D., Lesko, N., Park, C. B., Cámara, Y., Shi, Y., Wibom, R., Hultenby, K., Gustafsson, C. M., and Larsson, N. G. (2009) Methylation of 12S rRNA is necessary for *in vivo* stability of the small subunit of the mammalian mitochondrial ribosome. *Cell Metab.* **9,** 386–397
11. He, X., Sun, C., Wang, F., Shan, A., Guo, T., Gu, W., Cui, B., and Ning, G. (2012) Peri-implantation lethality in mice lacking the PGC-1-related coactivator protein. *Dev. Dyn.* **241,** 975–983
12. Scarpulla, R. C. (2008) Transcriptional paradigms in mammalian mitochondrial biogenesis and function. *Physiol. Rev.* **88,** 611–638
13. Scarpulla, R. C. (2012) Nucleus-encoded regulators of mitochondrial function: Integration of respiratory chain expression, nutrient sensing and metabolic stress. *Biochim. Biophys. Acta* **1819,** 1088–1097
14. Andersson, U., and Scarpulla, R. C. (2001) Pgc-1-related coactivator, a novel, serum-inducible coactivator of nuclear respiratory factor 1-dependent transcription in mammalian cells. *Mol. Cell Biol.* **21,** 3738–3749
15. Gleyzer, N., and Scarpulla, R. C. (2011) PGC-1-related coactivator (PRC), a sensor of metabolic stress, orchestrates a redox-sensitive program of inflammatory gene expression. *J. Biol. Chem.* **286,** 39715–39725
16. Gleyzer, N., and Scarpulla, R. C. (2013) Activation of a PGC-1-related coactivator (PRC)-dependent inflammatory stress program linked to apoptosis and premature senescence. *J. Biol. Chem.* **288,** 8004–8015
17. Wu, Z., Puigserver, P., Andersson, U., Zhang, C., Adelmant, G., Mootha, V., Troy, A., Cinti, S., Lowell, B., Scarpulla, R. C., and Spiegelman, B. M. (1999) Mechanisms controlling mitochondrial biogenesis and function through the thermogenic coactivator PGC-1. *Cell* **98,** 115–124
18. Gohil, V. M., Sheth, S. A., Nilsson, R., Wojtovich, A. P., Lee, J. H., Perocchi, F., Chen, W., Clish, C. B., Ayata, C., Brookes, P. S., and Mootha, V. K.

(2010) Nutrient-sensitized screening for drugs that shift energy metabolism from mitochondrial respiration to glycolysis. *Nat. Biotechnol.* **28,** 249–255

19. Yin, X., Giap, C., Lazo, J. S., and Prochownik, E. V. (2003) Low molecular weight inhibitors of Myc-Max interaction and function. *Oncogene* **22,** 6151–6159

20. Fiol, C. J., Mahrenholz, A. M., Wang, Y., Roeske, R. W., and Roach, P. J. (1987) Formation of protein kinase recognition sites by covalent modification of the substrate: molecular mechanism for the synergistic action of casein kinase II and glycogen synthase kinase 3. *J. Biol. Chem.* **262,** 14042–14048

21. Manning, B. D., and Cantley, L. C. (2007) AKT/PKB signaling: navigating downstream. *Cell* **129,** 1261–1274

22. Gregory, M. A., Qi, Y., and Hann, S. R. (2003) Phosphorylation by glycogen synthase kinase-3 controls c-Myc proteolysis and subnuclear localization. *J. Biol. Chem.* **278,** 51606–51612

23. Yeh, E., Cunningham, M., Arnold, H., Chasse, D., Monteith, T., Ivaldi, G., Hahn, W. C., Stukenberg, P. T., Shenolikar, S., Uchida, T., Counter, C. M., Nevins, J. R., Means, A. R., and Sears, R. (2004) A signalling pathway controlling c-Myc degradation that impacts oncogenic transformation of human cells. *Nat. Cell Biol.* **6,** 308–318

24. Marsell, R., Sisask, G., Nilsson, Y., Sundgren-Andersson, A. K., Andersson, U., Larsson, S., Nilsson, O., Ljunggren, O., and Jonsson, K. B. (2012) GSK-3 inhibition by an orally active small molecule increases bone mass in rats. *Bone* **50,** 619–627

25. Guha, M., Fang, J. K., Monks, R., Birnbaum, M. J., and Avadhani, N. G. (2010) Activation of Akt is essential for the propagation of mitochondrial respiratory stress signaling and activation of the transcriptional coactivator heterogeneous ribonucleoprotein A2. *Mol. Biol. Cell* **21,** 3578–3589

26. Hirai, H., Sootome, H., Nakatsuru, Y., Miyama, K., Taguchi, S., Tsujioka, K., Ueno, Y., Hatch, H., Majumder, P. K., Pan, B. S., and Kotani, H. (2010) MK-2206, an allosteric Akt inhibitor, enhances antitumor efficacy by standard chemotherapeutic agents or molecular targeted drugs *in vitro* and *in vivo*. *Mol. Cancer Ther.* **9,** 1956–1967

27. Cohen, I., Idan, C., Rider, P., Peleg, R., Vornov, E., Elena, V., Tomas, M., Martin, T., Tudor, C., Cicerone, T., Wegner, M., Mareike, W., Brondani, L., Lydia, B., Freudenberg, M., *et al.* (2015) IL-1α is a DNA damage sensor linking genotoxic stress signaling to sterile inflammation and innate immunity. *Sci. Rep.* **5,** 14756

28. Laberge, R. M., Sun, Y., Orjalo, A. V., Patil, C. K., Freund, A., Zhou, L., Curran, S. C., Davalos, A. R., Wilson-Edell, K. A., Liu, S., Limbad, C., Demaria, M., Li, P., Hubbard, G. B., Ikeno, Y., Javors, M., *et al.* (2015) MTOR regulates the pro-tumorigenic senescence-associated secretory phenotype by promoting IL1A translation. *Nat. Cell Biol.* **17,** 1049–1061

29. Kim, W., Bennett, E. J., Huttlin, E. L., Guo, A., Li, J., Possemato, A., Sowa, M. E., Rad, R., Rush, J., Comb, M. J., Harper, J. W., and Gygi, S. P. (2011) Systematic and quantitative assessment of the ubiquitin-modified proteome. *Mol. Cell* **44,** 325–340

30. Flick, K., and Kaiser, P. (2012) Protein degradation and the stress response. *Semin. Cell Dev. Biol.* **23,** 515–522

31. Sears, R., Nuckolls, F., Haura, E., Taya, Y., Tamai, K., and Nevins, J. R. (2000) Multiple Ras-dependent phosphorylation pathways regulate Myc protein stability. *Genes Dev.* **14,** 2501–2514

32. Rigbolt, K. T., Prokhorova, T. A., Akimov, V., Henningsen, J., Johansen, P. T., Kratchmarova, I., Kassem, M., Mann, M., Olsen, J. V., and Blagoev, B. (2011) System-wide temporal characterization of the proteome and phosphoproteome of human embryonic stem cell differentiation. *Sci. Signal.* **4,** rs3

33. Hers, I., Vincent, E. E., and Tavaré, J. M. (2011) Akt signalling in health and disease. *Cell Signal.* **23,** 1515–1527

34. Wang, H., and Morais, R. (1997) Up-regulation of nuclear genes in response to inhibition of mitochondrial DNA expression in chicken cells. *Biochim. Biophys. Acta* **1352,** 325–334

35. Biswas, G., Guha, M., and Avadhani, N. G. (2005) Mitochondria-to-nucleus stress signaling in mammalian cells: nature of nuclear gene targets, transcription regulation, and induced resistance to apoptosis. *Gene* **354,** 132–139

36. Gohil, V. M., Zhu, L., Baker, C. D., Cracan, V., Yaseen, A., Jain, M., Clish, C. B., Brookes, P. S., Bakovic, M., and Mootha, V. K. (2013) Meclizine inhibits mitochondrial respiration through direct targeting of cytosolic phosphoethanolamine metabolism. *J. Biol. Chem.* **288,** 35387–35395

37. Weber, A., Wasiliew, P., and Kracht, M. (2010) Interleukin-1 (IL-1) pathway. *Sci. Signal.* **3,** cm1

38. Luheshi, N. M., Rothwell, N. J., and Brough, D. (2009) Dual functionality of interleukin-1 family cytokines: implications for anti-interleukin-1 therapy. *Br. J. Pharmacol.* **157,** 1318–1329

39. Cohen, I., Rider, P., Carmi, Y., Braiman, A., Dotan, S., White, M. R., Voronov, E., Martin, M. U., Dinarello, C. A., and Apte, R. N. (2010) Differential release of chromatin-bound IL-1α discriminates between necrotic and apoptotic cell death by the ability to induce sterile inflammation. *Proc. Natl. Acad. Sci. U.S.A.* **107,** 2574–2579

40. Kang, C., Xu, Q., Martin, T. D., Li, M. Z., Demaria, M., Aron, L., Lu, T., Yankner, B. A., Campisi, J., and Elledge, S. J. (2015) The DNA damage response induces inflammation and senescence by inhibiting autophagy of GATA4. *Science* **349,** aaa5612

41. Rohban, S., and Campaner, S. (2015) Myc induced replicative stress response: How to cope with it and exploit it. *Biochim. Biophys. Acta* **1849,** 517–524

42. Hart, L. S., Cunningham, J. T., Datta, T., Dey, S., Tameire, F., Lehman, S. L., Qiu, B., Zhang, H., Cerniglia, G., Bi, M., Li, Y., Gao, Y., Liu, H., Li, C., Maity, A., *et al.* (2012) ER stress-mediated autophagy promotes Myc-dependent transformation and tumor growth. *J. Clin. Invest.* **122,** 4621–4634

43. Dey, S., Tameire, F., and Koumenis, C. (2013) PERK-ing up autophagy during MYC-induced tumorigenesis. *Autophagy* **9,** 612–614

44. Campaner, S., and Amati, B. (2012) Two sides of the Myc-induced DNA damage response: from tumor suppression to tumor maintenance. *Cell Div.* **7,** 6

45. Benassi, B., Fanciulli, M., Fiorentino, F., Porrello, A., Chiorino, G., Loda, M., Zupi, G., and Biroccio, A. (2006) c-Myc phosphorylation is required for cellular response to oxidative stress. *Mol. cell* **21,** 509–519

46. Whitfield, J. R., and Soucek, L. (2012) Tumor microenvironment: becoming sick of Myc. *Cell. Mol. Life Sci.* **69,** 931–934

47. Shchors, K., Shchors, E., Rostker, F., Lawlor, E. R., Brown-Swigart, L., and Evan, G. I. (2006) The Myc-dependent angiogenic switch in tumors is mediated by interleukin 1β. *Genes Dev.* **20,** 2527–2538

48. Yoon, J. C., Ling, A. J., Isik, M., Lee, D. Y., Steinbaugh, M. J., Sack, L. M., Boduch, A. N., Blackwell, T. K., Sinclair, D. A., and Elledge, S. J. (2014) GLTSCR2/PICT1 links mitochondrial stress and Myc signaling. *Proc. Natl. Acad. Sci. U.S.A.* **111,** 3781–3786

49. Lin, C. Y., Lovén, J., Rahl, P. B., Paranal, R. M., Burge, C. B., Bradner, J. E., Lee, T. I., and Young, R. A. (2012) Transcriptional amplification in tumor cells with elevated c-Myc. *Cell* **151,** 56–67

50. Ward, P. S., and Thompson, C. B. (2012) Metabolic reprogramming: a cancer hallmark even warburg did not anticipate. *Cancer Cell* **21,** 297–308

51. Grivennikov, S. I., and Karin, M. (2010) Inflammation and oncogenesis: a vicious connection. *Curr. Opin. Genet. Dev.* **20,** 65–71

52. Mahajan, K., and Mahajan, N. P. (2012) PI3K-independent AKT activation in cancers: a treasure trove for novel therapeutics. *J. Cell Physiol.* **227,** 3178–3184

53. Kennedy, S. G., Wagner, A. J., Conzen, S. D., Jordán, J., Bellacosa, A., Tsichlis, P. N., and Hay, N. (1997) The PI 3-kinase/Akt signaling pathway delivers an anti-apoptotic signal. *Genes Dev.* **11,** 701–713

54. Brunet, A., Bonni, A., Zigmond, M. J., Lin, M. Z., Juo, P., Hu, L. S., Anderson, M. J., Arden, K. C., Blenis, J., and Greenberg, M. E. (1999) Akt promotes cell survival by phosphorylating and inhibiting a Forkhead transcription factor. *Cell* **96,** 857–868

55. Molife, L. R., Yan, L., Vitfell-Rasmussen, J., Zernhelt, A. M., Sullivan, D. M., Cassier, P. A., Chen, E., Biondo, A., Tetteh, E., Siu, L. L., Patnaik, A., Papadopoulos, K. P., de Bono, J. S., Tolcher, A. W., and Minton, S. (2014) Phase 1 trial of the oral AKT inhibitor MK-2206 plus carboplatin/paclitaxel, docetaxel, or erlotinib in patients with advanced solid tumors. *J. Hematol. Oncol.* **7,** 1

56. Hudis, C., Swanton, C., Janjigian, Y. Y., Lee, R., Sutherland, S., Lehman, R., Chandarlapaty, S., Hamilton, N., Gajria, D., Knowles, J., Shah, J., Shannon, K., Tetteh, E., Sullivan, D. M., Moreno, C., *et al.* (2013) A phase 1 study evaluating the combination of an allosteric AKT inhibitor (MK-2206) and trastuzumab in patients with HER2-positive solid tumors. *Breast Cancer Res.* **15,** R110

57. Wu, D., and Pan, W. (2010) GSK3: a multifaceted kinase in Wnt signaling. *Trends Biochem. Sci.* **35,** 161–168

58. Gugneja, S., and Scarpulla, R. C. (1997) Serine phosphorylation within a concise amino-terminal domain in nuclear respiratory factor 1 enhances DNA binding. *J. Biol. Chem.* **272,** 18732–18739

59. Vercauteren, K., Gleyzer, N., and Scarpulla, R. C. (2008) PGC-1-related coactivator complexes with HCF-1 and NRF-2β in mediating NRF-2(GABP)-dependent respiratory gene expression. *J. Biol. Chem.* **283,** 12102–12111